EurJIC
European Journal of Inorganic Chemistry

Research Article
doi.org/10.1002/ejic.202400228

Chemistry Europe
European Chemical Societies Publishing

www.eurjic.org

TMPA-based Cavitary Cobalt (II) Funnel Complexes

Nicolas Nyssen,[a, c] Abdullah Abudayyeh,[a] Fedor Zhurkin,[d] Pamela Aoun,[a] Aleksandar Višnjevac,*[b] Benoit Colasson,[a] Ivan Jabin,[c] and Olivia Reinaud*[a]

The synthesis of a series of mononuclear, dicationic Co^{II} funnel complexes is reported herein. Three ligands **Calix-TMPA^{X}** present a calix[6]arene cone closed at its small rim by a *tris*(2-pyridylmethyl)amine (TMPA) unit and differ by the nature of three cavity walls, anisole, phenol or quinone. The X-ray diffraction structure of [Co^{II}(MeCN)**Calix-TMPA^{OMe}**]$(ClO_4)_2$ displays a trigonal bipyramidal geometry, with Co bound to all 4 nitrogen atoms of the TMPA cap, and to one MeCN guest molecule buried inside the calixarene cavity. All complexes were fully characterized in solution as high spin 5-coordinate species using various techniques, including ^{1}H NMR spectroscopy. For comparison purpose, an analogous Co^{II} complex based on the **TMPA^{CH2OH}** ligand, devoid of a calixarene core, was synthetized. Its X-ray structure shows a dicationic 7-coordinate cobalt(II) center in the N_4O_3 environment provided by the ligand, leaving no space for exogenous ligand binding. This contrasts with the 5-coordinate complexes obtained with the calix-ligands that allow guest-ligand binding and exchange. A brief overview of the coordination properties of the calix-complexes, compared to those obtained with TMPA ligands, devoid of a cavity, highlights major differences in terms of complexation kinetics, geometry, coordination to the labile site, anion affinity, nuclearity, and stability.

Introduction

It is now well recognized that supramolecular interactions play a crucial role in controlling the reactivity of a metal center embedded within a proteic cavity. Indeed, hydrogen-bonding, dipole interactions, inductive effects, water molecule entrapping, and the hydrophobic effect have all been shown to drastically affect the stability, lability, and catalytic properties of the metal ion(s) embedded within the active site. One area of interest in bioinorganic chemistry is the supramolecular control of metal complexes in a biomimetic environment. The use of supramolecular chemistry associated to biomimetic coordination chemistry aims at replicating some aspects of the metal-containing active sites found in metalloenzymes. One strategy involves the confinement of a metal center in a macrocyclic structure that is open to the solvent, thus allowing and controlling guest ligand exchange.[1–2] Ligands based on calix[6]arenes covalently capped at the small rim by a nitrogen core mimic the polyhistidine-rich environment found in metalloenzymes.[3] The calix[6]arene core surrounding the guest ligand site allows for a very fine tuning of the second coordination sphere of the metal center. Out of the six aromatic units forming a conic cavity, three are used to connect the nitrogen-rich site that caps the small rim, whereas the three others can bring various functionalities in the near environment of the metal ion bound to the nitrogen cap, such as anisole, phenol, or quinone.[4]

Biomimetic Zn^{II} and $Cu^{II/I}$ complexes of calix[6]arenes capped by a TMPA (tris(2-pyridylmethyl)amine) unit have been previously reported.[1–5] The complexes allowed for the exploration of the specific coordination properties of these metal ions when embedded in macrocyclic architectures. Thermodynamics and kinetics of guest-ligand exchange were explored in depth by NMR spectroscopy with the Zn^{II} complexes,[4,6] while $Cu^{II/I}$ complexes were studied as redox centers for O_2 activation.[7] Wanting to explore reductive redox processes involving proton-coupled multiple electron transfer, we decided to investigate the coordination of Co^{II} to these calixarene ligands. Indeed, many Co complexes based on poly-aromatic aza ligands were reported to display good to excellent activity in reductive catalytic processes.[8–15] With TMPA ligands specifically, Co^{II} complexes were described as active for electro- and photocatalytic reduction of small molecules such as CO_2[16–19] and O_2[20] along with H_2 evolution.[21–26]

Most of the reported Co^{II} complexes coordinated to a TMPA unit, devoid of cavitary control, are mono-cationic species due to their propensity to bind anions: some are 5-coordinate with

[a] Dr. N. Nyssen, Dr. A. Abudayyeh, Dr. P. Aoun, Prof. B. Colasson, Prof. O. Reinaud
Université Paris Cité, CNRS
Laboratoire de Chimie et de Biochimie Pharmacologiques et Toxicologiques
F-75006 Paris, France
E-mail: Olivia.Reinaud@u-paris.fr

[b] Dr. A. Višnjevac
Physical Chemistry Division
Ruđer Bošković Institute
Bijenička 54, HR-10000 Zagreb, Croatia
E-mail: aleksandar.visnjevac@irb.hr

[c] Dr. N. Nyssen, Prof. I. Jabin
Laboratoire de Chimie Organique
Université libre de Bruxelles
Avenue F. D. Roosevelt, 50 - 1050 Bruxelles, Belgium

[d] Dr. F. Zhurkin
Present address:
Institute of Chemistry for Life and Health sciences, CSB2D
Chimie ParisTech, PSL Research University
75005 Paris, France

Supporting information for this article is available on the WWW under https://doi.org/10.1002/ejic.202400228

Research Article
doi.org/10.1002/ejic.202400228

an anion (such as I^-, Cl^-, Br^-, TfO^-, SCN^- or carboxylates) bound at the apical site of the trigonal pyramid or 6-coordinate with anionic donors.[16,20, 27–35] Many complexes have been reported with bidentate ligands such as hydroxamates or carboxylates.[36–38] With neutral ligands, only few well-defined complexes were reported, such as nitrilo dicationic complexes.[24,39] Some bridged TMPA-based Co complexes have also been described. However, the Co cations are present in a higher oxidation state. Dinuclear diamond bridged (μO^-,μO^-) Co^{III} complexes were reported for C–H activation.[40–41]

All these data encouraged us to explore the coordination chemistry of Co^{II} when constrained in the macrocyclic structure provided by the calix[6]arene core capped by the TMPA ligand. The idea is that the cone-like macrocycle would constrain the metal ion in a mononuclear state with a proximal environment defined by the calixarene and its functionalization pattern (Figure 1). Importantly, this type of cavity, although capped at the small rim of the calixarene core by the nitrogenous donor, would remain open to the solvent at the other side (large rim), allowing guest ligand (G) exchange, essential for catalysis. Variation of the functionalization pattern (X, see Figure 1) of 3 out of the 6 aromatic units at the small rim would allow fine-tuning of the environment around the embedded metal center. The present article reports the synthesis of these calixarene-based Co^{II} complexes and explores the general trends of their chemical behavior in terms of coordination environment, stability, and ligand exchange compared to their TMPA analogs without the calixarene moiety.

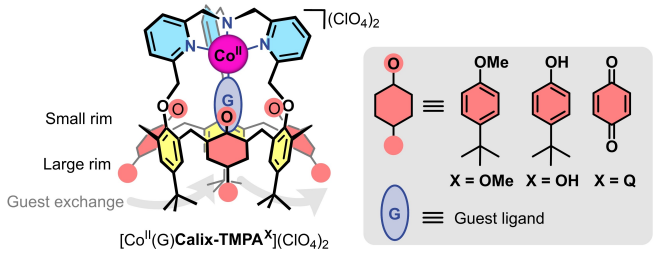

[Co^{II}(G)**Calix-TMPA^X**]$(ClO_4)_2$

Figure 1. Host-guest properties of targeted calixarene-based complexes, [Co^{II}(G)**Calix-TMPA^X**]$(ClO_4)_2$ (**X** = OMe, OH, Q).

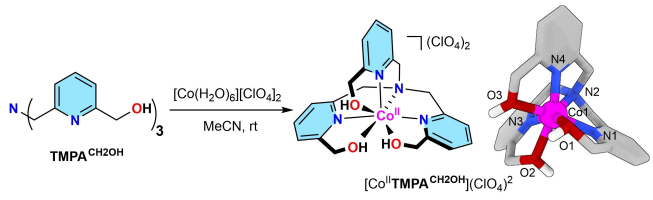

Figure 2. Synthetic scheme (left) and XRD structure (right) of [Co^{II}**TMPA^{CH2OH}**]$(ClO_4)_2$. H atoms (except OH ones) and counter ions are omitted for clarity. Bond lengths (Å): N1-CO1 2.092(4), N2-CO1 2.298(3), N3-CO1 2.111(3), N4-CO1 2.107(3), O1-CO1 2.271(3), O2-CO1 2.233(3), O3-CO1 2.266(3). Bond angles (°): N1-CO1-N4 110.17(13), N1-CO1-N3 113.73(13), N1-CO1-O2 89.57(14), N4-CO1-O3 73.15(11), N3-CO1-O3 88.66(12), O2-CO1-O3 80.58(12), N1-CO1-O1 73.36(13), N4-CO1-O1 88.64(12), N3-CO1-O1 150.44(13), O2-CO1-O1 78.91(13), O3-CO1-O1 78.73(12), N1-CO1-N2 74.04(13), N4-CO1-N2 73.67(11), N3-CO1-N2 73.28(12), O2-CO1-N2 131.65(12), O3-CO1-N2 131.45(11), O1-CO1-N2 134.32(13).

Results and Discussion

For the sake of comparison with calixarene-based TMPA complexes, the Co^{II} complex of ligand **TMPA^{CH2OH}** was first synthetized (Figure 2). Reacting one equivalent of cobalt(II) perchlorate hexahydrate with the ligand under an inert atmosphere in MeCN at room temperature led almost immediately to a dark pink solution, from which single crystals suitable for X-ray diffraction analysis were obtained by diethyl ether diffusion. The XRD structure shows a Co^{II} center in a hepta-coordinate environment in a distorted capped trigonal prismatic mode (Figure 2). The three hydroxymethyl arms occupy the basal positions of the distorted prism and are relatively weekly bound, as indicated by the long Co–O distances (> 2.2 Å). The longer bond to the tertiary amine nitrogen N2 (2.30 Å) caps the expanded triangular face formed by Co–N bonds to the pyridyl nitrogen atoms N1, N3 and N4, at the apex of the distorted prism. A similar coordination pattern was previously reported for the Mn^{II} complex of the very same ligand.[42]

In solution, the complex was characterized by ^1H NMR spectroscopy in CD_3CN. The C_{3v} symmetry of the complex is reflected by the presence of three peaks for the coordinated pyridyl donors, and two peaks for the methylene protons. The formers are the most low-field shifted ($\delta = 167.1$, 53.2 and 41.0 ppm), in accordance with their shorter coordination bonds. Comparatively, the methylene protons connecting the four other donors are less shifted ($\delta = 12.43$ and 10.47 ppm), lying at longer distances from the metal center. The UV-VIS absorption spectrum displayed three bands at 486, 686 and 1000 nm with $\varepsilon \leq 50\ M^{-1}cm^{-1}$, which is consistent with a high coordination number.[43–44] The characterization was completed with the IR spectrum, confirming the presence of ClO_4^- counter anions ($\delta =$ 620 cm^{-1}), and HRMS (see the SI).

The three Co^{II}**Calix-TMPA^X** complexes were synthesized in good yields (> 80 %) in MeCN by reacting ligands **Calix-TMPA^X** with cobalt(II) perchlorate hexahydrate (Figure 3). The reaction required extensive heating to achieve full complexation of the ligands, yielding [Co(MeCN)**Calix-TMPA^X**][ClO_4]$_2$. This stands in strong contrast with TMPA ligands deprived of a calixarene core, for which complexation proceeds within minutes at room temperature. Furthermore, the reaction time varied with the nature of the functionalization of the calix-core. With ligands **Calix-TMPA^{OMe}** and **Calix-TMPA^Q**, overnight heating at 80 °C was required to obtain full complexation, while with **Calix-**

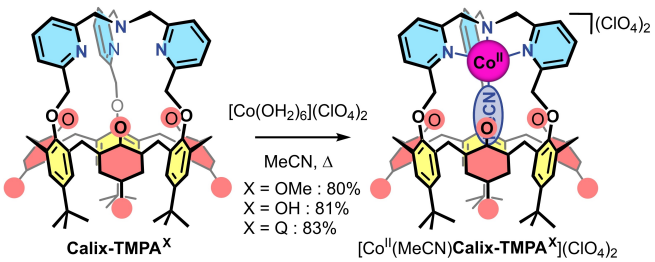

Figure 3. Synthesis of calixarene-based complexes, [Co^{II}(MeCN)**Calix-TMPA^X**]$(ClO_4)_2$ (**X** = OMe, OH, Q).

Research Article
doi.org/10.1002/ejic.202400228

TMPA^{OH}, the reaction was complete after only 6 hours at 80 °C. In each case, the reaction of **Calix-TMPA^{X}** with the metal salt first led to the mono-protonation of the TMPA cap, and heating the solution was necessary to displace the equilibria {formally **TMPA**H^{+} + Co(OH)$^{+}$ ⇆ TMPA + Co(OH$_2$)$^{2+}$ ⇆ **TMPA**Co^{2+} + H_2O} in favor of the metal complex. Such a slow kinetic for the complexation process is obviously related to the restricted access to the TMPA site due to constraints imposed by its connection to the calixarene core. The relatively faster process observed with **Calix-TMPA^{OH}** can be ascribed to transient assistance of the oxygen donors phenol functions (**X = OH**) present at the small rim of the calixarene, that are less bulky than those of the anisole units (**X = OMe**) and better donor than those of the quinones (**X = Q**).[4] All three Co^{II} complexes obtained with ligands **Calix-TMPA^{X}** are highly stable either in solution (at 80 °C, for hours) or in the solid state (months). In contrast, the complex synthetized with the simple **TMPA** ligand, [Co^{II}(MeCN)**TMPA**](ClO$_4$)$_2$,[39] decomposed in the solid state within a few weeks.

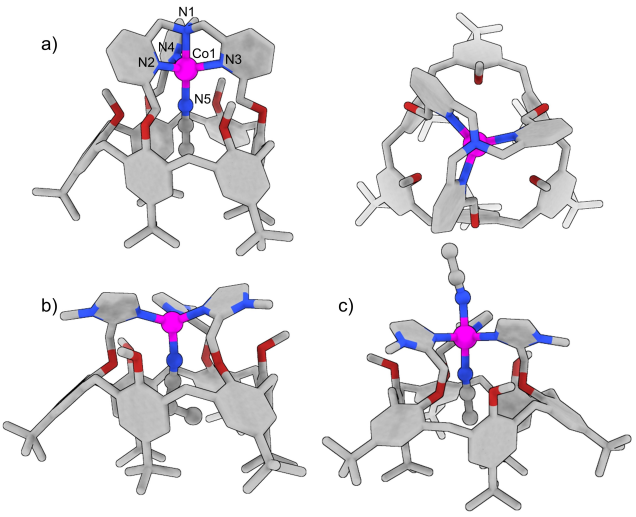

Figure 4. XRD structures of Co^{II} complexes obtained with calix[6]arene-based ligands providing a TMPA or a tris(imidazole) coordination site. H atoms and counter ions are omitted for clarity. a) side view and top views of [Co^{II}(MeCN)**Calix-TMPA^{OMe}**]$^{2+}$. Bond lengths (Å): N1-Co1 2.097(10), N2-Co1 2.157(10), N3-Co1 2.154(9), N4-Co1 2.149(9), N5-Co1 2.065(10). Bond angles (°): N5-Co1-N1 179.1(3), N5-Co1-N3 102.0(3), N1-Co1-N3 78.9(4), N5-Co1-N2 101.1(3), N1-Co1-N2 78.6(4), N3-Co1-N2 117.4(3), N5-Co1-N4 102.4(3), N1-Co1-N4 78.9(4), N3-Co1-N4 117.6(4), N2-Co1 N4-112.6(4). b) [Co^{II}(EtCN)**Calix-tris(Imme)**]$^{2+}$. c) [Co^{II}(MeCN)$_2$**Calix-tris(Imme)**]$^{2+}$.[45]

Single crystals suitable for X-ray diffraction analysis were obtained for [Co(MeCN)**Calix-TMPA^{OMe}**][ClO$_4$]$_2$ by diethyl ether diffusion into a solution of the complex in MeCN. The XRD structure reveals a 5-coordinate environment for the Co^{II} center due to its coordination to the TMPA cap, which, hence, acts as a tetradentate ligand, and one intra-cavity bound acetonitrile molecule (Figure 4 Top). The latter sits in the heart of the calixarene cavity, along the non-crystallographic C_3 axis of the trigonal bipyramidal (TBP) structure. The bipyramid is slightly compressed as the tertiary nitrogen of TMPA and the MeCN guest ligand lie at slightly shorter distances than the pyridyl donors, which contrasts with [Co^{II}(MeCN)**TMPA**]$^{2+}$ complexes without a calixarene cavity attached (see Table 1), displaying an elongated TBP geometry.[19,27,39] Such an environment also differs strongly from complex [Co^{II}**TMPA^{CH2OH}**]$^{2+}$ where the oxygen donors are all bound, with no MeCN solvent coordi-

Table 1. Comparative data of Co^{II} complexes.

Complex	λ_{max} (nm) (ε / M^{-1}cm^{-1})	Bond distances (Å) N_5 = MeCN	τ[46]	μ_{eff} (μ_B)
[Co(MeCN)TMPA][ClO$_4$]$_2$ [39]	472 (85), 552 (72) in MeCN	Co-N$_{ap}$: 2.177 Co-N$_{Py}$: 2.04-2.05 Co-N$_{MeCN}$: 2.05	0.94	4.2
[Co(G)(Calix-*tris*(Imme))][ClO$_4$]$_2$ [45]	G = H_2O in CH_2Cl_2: 523 (230), 564 (336), 592 (339)	G = MeCN: Co-N$_{Im}$: 1.996, 2.002, 2.003 Co-N$_{MeCN\ endo}$: 1.956		4.6
[Co(MeCN)$_2$(Calix-*tris*(Imme))][ClO$_4$]$_2$ [45]	530 (170), 566 (260), 595 (230) in MeCN/CH_2Cl_2	Co-N$_{Im}$: 2.046, 2.053, 2.061 (av.: 2.053) Co-N$_{MeCN\ endo}$: 2.078 Co-N$_{MeCN\ exo}$: 2.171	0.69	/
[Co(TMPA^{CH2OH}][ClO$_4$]$_2$	486 (50), 686 (5), 1000 (11) in MeCN	Co-N$_{ap}$: 2.298 Co-N$_{Py}$: 2.092, 2.111, 2.107 Co-OH: 2.271, 2.233, 2.266		4.6
[Co(MeCN)(Calix-TMPA^{OMe})][ClO$_4$]$_2$	346 (367), 484 (89), 618 (67) in MeCN	Co-N$_{ap}$: 2.09 Co- N$_{py}$: 2.16, 2.14, 2.15 Co-N$_{MeCN}$: 2.04	1.05	3.8
[Co(MeCN)(Calix-TMPA^{OH})][ClO$_4$]$_2$	343 (556), 478 (122), 613 (93) in MeCN			3.5
[Co(MeCN)(Calix-TMPA^{Q})][ClO$_4$]$_2$	369 (1849), 475 (733), 603 (256) in MeCN			3.8
[Co(H_2O)(Calix-TMPA^{OH})][ClO$_4$]$_2$	453 (152), 480 (166), 602 (55), 635 (72) in acetone			

Research Article
doi.org/10.1002/ejic.202400228

nated. Such a difference stems from constraints imposed by the calixarene skeleton that maintains the oxygen atoms at distances longer than 4 Å, whereas protecting the apical site for guest binding in the center of the cavity. This cobalt complex also differs from the one we previously reported with a related calix[6]arene-based ligand, namely **Calix-tris(Imme)**, presenting three imidazolyl donors connected through the same methylene linkers to the phenolic units.[45] With the cobalt complex of **Calix-tris(Imme)**, two different coordination sites were available for exogenous ligands. Indeed, beside the *endo*-coordinated guest ligand, a second site remained open to the solvent, in the *exo*-apical position. The latter could be occupied or not, leading to a Co^{II} center that can switch from a 4-coordinate tetrahedral environment to a 5-coordinate, distorted and elongated TBP environment, depending on the conditions (Figure 4 Bottom and Table 1). With **Calix-TMPA^{OMe}**, the apical *exo*-position is occupied by the tertiary nitrogen atom of the TMPA cap that prevents *exo*-binding of extra-donors along the C_3 axis. Another important difference with the *tris*(imidazole) system stems from the different conformation adopted by the calixarene core. In both cases, the aromatic units adopt an alternate in/out orientation relative to the center of the cavity. However, whereas the oxygen atoms connected to the aza-donors are projected toward the inner face of the cavity walls for imidazoles, they are constrained in the opposite direction (*ie.* toward the outer face) for the rigid TMPA cap. As a result, the oxygen lone pairs of the anisole units are oriented toward the metal center when bound to the 3 imidazole arms, whereas they point toward the solvent, away from the metal center with TMPA. Finally, the presence of the three methyl groups prevents a change in orientation of the oxygen lone pairs, hampering any assistance during the coordination of the Co^{II} cation. This rotation becomes possible with the phenol units of **Calix-TMPA^{OH}** and explains, as observed with Zn^{II}, the fastest kinetics of complexation.

Lastly, the hereby presented crystal structure resembles the one obtained with Cu^{II} (5-coordinate center with MeCN as a guest ligand), although bond distances differ significantly: longer Cu-N_{Py} bond (2.30 vs 2.15 Å) and shorter Cu-N_{MeCN} bond (1.92 vs 2.07 Å).[5]

The three [Co^{II}(MeCN)**Calix-TMPA^{X}**]$(ClO_4)_2$ complexes were characterized in solution by ^{1}H NMR spectroscopy (Figure 5). The three spectra show two H_{py} signals at low-field, whereas the third H_{py} is high-field shifted, below 0 ppm. All the other signals are located within the 0 to 8 ppm window. The similarity of the ^{1}H NMR signatures and chemical shifts advocates for very similar structures and is in accordance with the above-depicted solid state C_{3v} symmetrical structure. It is to be noted that none of the methylene protons close to the Co^{II} center (NCH_2, OCH_2) could be detected, probably because of extensive broadening of the corresponding signals due to the paramagnetism of the metal ion.

Interestingly, in the case of ligand **Calix-TMPA^{OMe}**, the coordination of a CH_3CN guest could be clearly evidenced in the ^{1}H NMR spectrum recorded in CD_3CN. Indeed, when the spectrum was recorded shortly after the preparation of the Co^{II} solution of the isolated complex dissolved in dry CD_3CN, an extra resonance at 26 ppm was detected (Figure 5). This resonance integrated for approximately 3 protons and gradually disappeared over time (after a few hours, see the SI). It could be unambiguously assigned to one equivalent of CH_3CN guest ligand, originating from the solvent used for the synthesis of the complex, which undergoes slow exchange with CD_3CN during ^{1}H NMR analyses. With **Calix-TMPA^{OH}** and **Calix-TMPA^{Q}**, the CH_3CN guest ligand could not be observed, which is explained by a much faster exchange rate. These observations qualitatively align with our previous studies with the analogous Zn^{II} complexes: very slow guest exchange in the case of **Calix-TMPA^{OMe}**, much faster with **Calix-TMPA^{OH}** and **Calix-TMPA^{Q}**. The mechanism of guest exchange has been the subject of in-depth kinetic studies with the diamagnetic Zn^{II} complexes.[6] They revealed the key role played by a single molecule of water (due to the presence of residual water in the solvent) that transiently binds to the metal center, thereby catalyzing the expulsion of the organic guest ligand.

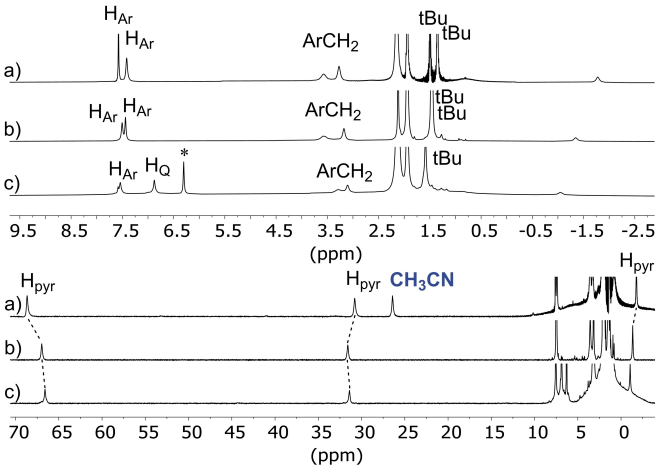

Figure 5. ^{1}H NMR of [Co^{II}(MeCN)**Calix-TMPA^{X}**]$(ClO_4)_2$ (500 MHz, 298 K) in CD_3CN. **X** = a) **OMe**, b) **OH**, c) **Q**. The NCH_2 and OCH_2 protons could not be detected. *1,1-2,2-$C_2H_2Cl_4$ used as an internal reference. The assignments were done by peak integration and comparison with the literature data (see ref. [39]).

The magnetic moments, measured by Evans method[47] (Table 1), indicate a high spin state for the three complexes in MeCN (S = 3/2).[48–50] The UV-VIS absorption spectra show the presence of two main bands in the visible region, at ca. 480 and 630 nm, with extinction coefficients of ca. 50–80 $M^{-1}cm^{-1}$ (Figure 6). These absorptions are typical for 5-coordinate Co^{II} complexes[43–44] and are clearly different from those exhibited by the 7-coordinate complex Co^{II}**TMPA^{CH2OH}**. IR spectra of the three complexes further confirmed the dicationic state of the cobalt ion, with two perchlorates as counterions (see the SI).

Finally, it is worth to note that when **Calix-TMPA^{OMe}** was reacted with $CoCl_2$ in MeCN, the same ^{1}H NMR signature was obtained as for the perchlorate complex. This indicates the formation of the dicationic [Co^{II}(MeCN)**Calix-TMPA^{OMe}**]$^{2+}$ species with, most probably, the associated formation of $CoCl_4^{2-}$ as counterion (see the SI). In contrast, the same reaction with ligand **TMPA** yields a monocationic complex with a chloride bound to the metal center.[28,51]

Research Article
doi.org/10.1002/ejic.202400228

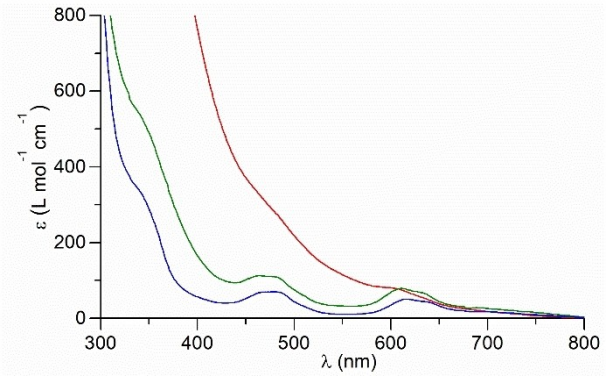

Figure 6. UV-Vis spectra stack of the [Co^{II}(MeCN)**Calix-TMPA^{X}**](ClO$_4$)$_2$ complexes in MeCN (0.9 mM); X = OMe: blue, X = OH: green, X = Q: red trace.

Aqua and DMF Complexes

Having noticed the exceptional stability of dicationic nitrilo-Co^{II} complexes within the calixarene core, we ought to synthesize and characterize other species. For this purpose, we chose the **Calix-TMPA^{OH}** ligand for which complexation and ligand exchange processes are faster than for the more sterically encumbered **Calix-TMPA^{OMe}** ligand. When **Calix-TMPA^{OH}** was reacted with cobalt(II) perchlorate hexahydrate in the poorly coordinating solvent acetone (instead of MeCN), a new complex was isolated. The corresponding ^{1}H NMR spectrum, recorded in acetone, showed resonances clearly different from those of the above-described MeCN complex in the same solvent (Figure 7). UV-vis, IR and mass spectra indicated the formation of a dicationic complex. By analogy to the Zn^{II} complex, we assumed that this dicationic complex is the aqua complex.[6] When aliquots of MeCN were added to an acetone solution of this complex, the ^{1}H NMR spectrum showed the formation of the corresponding MeCN complex. When DMF was added instead of MeCN, a new signature was obtained. By comparison of the three different spectra, peaks at 30.2 and 39.2 ppm could be attributed to the methyl groups of the coordinated DMF molecule sitting inside the cavity [for comparison, δ(MeCN) = 29.5 ppm in the same solvent, Figure 7]. A titration experiment of the DMF complex by MeCN showed a fast exchange process

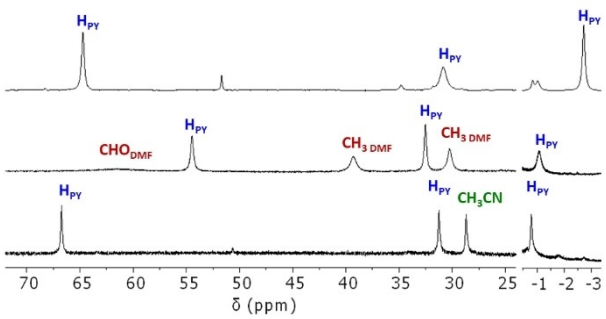

Figure 7. ^{1}H NMR spectra of [Co(G)**Calix-TMPA^{OH}**](ClO$_4$)$_2$ in acetone-d$_6$: From Top to Bottom: As synthesized in acetone: G = H$_2$O; After addition of DMF : G = DMF; As synthesized in MeCN: G = MeCN.

at the experiment time scale, but slow at the NMR shift time scale. Relative integration of the peaks corresponding to the various species in solution yielded a relative affinity of $K_{MeCN/DMF}$ of the Co^{II} center of 8 ± 1 (see the SI). This highlights a higher affinity for MeCN than for DMF, in spite of the fact that it is a less σ-donating ligand. A similar value was previously reported for the Cu^{II} complex of **Calix-TMPA^{OMe}** ($K_{MeCN/DMF}$ = 3), and was attributed to the exceptional shape complementarity of the calixarene core and the linear MeCN guest.[1]

Conclusions

Herein, we have described the synthesis and full characterization of four new Co^{II} complexes, namely [Co^{II}**TMPA^{CH2OH}**](ClO$_4$)$_2$, and [Co^{II}(G)**Calix-TMPA^{X}**](ClO$_4$)$_2$ with the anisole (X = OMe), phenol (X = OH) and quinone (X = Q) derivatives of the calix[6]arene-based ligands. All complexes are dicationic, associated to two perchlorate counter ions. When isolated from acetonitrile, the calix-complexes present a nitrile guest ligand that is strongly bound to the metal center, in the heart of the calixarene cavity. When synthetized in a poorly coordinating solvent such as acetone, the corresponding aqua-complex is isolated. In solution, the water guest can be readily displaced by MeCN or DMF that nicely fills the calixarene cavity. The 5-coordinate environment is maintained despite the presence of six oxygen donors on the calixarene ligands. This contrasts with the hepta-coordinate [Co^{II}**TMPA^{CH2OH}**]$^{2+}$ complex for which all three oxygen donors are bound to the metal ion, leaving no space available for acetonitrile binding. Such a coordination control is obviously due to the presence of the calixarene core that maintains all the oxygen donors at remote distance from the metal center (more than 4 Å).

To sum up, the coordination behavior of the calix-complexes showed number of differences with the Co^{II} complexes based on simple TMPA ligands, devoid of a calixarene cavity:

- *Complexation* – Whereas coordination of Co^{II} to **TMPA** occurs almost instantaneously in acetonitrile, full complexation to calix-ligands required extensive heating for several hours. Such a slow kinetic is explained by the restricted access to the nitrogen donors that are oriented toward the center of the cavity to which they are connected.
- *Stability* – All Co^{II} complexes herein characterized with ligands **Calix-TMPA^{X}** are highly stable both, in solution or in the solid state. In contrast, the complex synthetized with the simple **TMPA** ligand, [Co^{II}(MeCN)**TMPA**](ClO$_4$)$_2$,[39] decomposed in the solid state within a few weeks.
- *Geometry* – in all cases, the Co^{II} center seats in a TBP geometry with a high spin state. However, whereas its bond to the apical *N*-donor of **TMPA** is much longer than the four others, it is the converse situation with **Calix-TMPA^{OMe}**: both apical donors display shorter bonds than the three pyridine residues.
- *Coordination at the labile site* - the Co^{II} ion embedded in the calix-ligands displays a much higher affinity for MeCN than for chloride. The calixarene provides not only an oxygen-rich

Research Article
doi.org/10.1002/ejic.202400228

environment around the coordination site that disfavors anion binding, but also a remarkable complementary size and shape for a linear ligand such as MeCN, as shown by a higher relative affinity compared to DMF. Such a coordination behavior contrasts with **TMPA** with no calixarene, whatever the substitution pattern is, as with these ligands, only few dicationic Co^{II} complexes have been reported.

– *Nuclearity* – In all conditions, the calix-complexes are maintained in a mono-nuclear state, due to the protection by the cavity surrounding the labile site. This also contrasts with **TMPA** complexes that display a high propensity to form dinuclear complexes by spontaneous deprotonation of water or in the presence of potentially bridging anions.

All in all, the high stability of the calix-complexes combined with the full control of the 2nd coordination sphere that is tunable by various functions: anisole, phenol, quinone, possibly acting as proton relay or electron reservoir, make them very promising for reductive catalysis, which we are currently exploring.

Experimental Section

Synthetic Procedures for the Co^{II} Complexes

[Co^{II}TMPA^{CH2OH}](ClO$_4$)$_2$

In a double-neck round bottom flask (25 mL), **TMPA^{CH2OH}** (53 mg, 139 μmol) was dissolved in de-oxygenated MeCN (3 mL). An acetonitrile solution (3 mL) of $[Co^{II}(H_2O)_6](ClO_4)_2$ (52 mg, 142 μmol) was then added under flow of Ar. The solution became dark pink, and was stirred for 30 min. at room temperature. Ether diffusion (10 mL) into the solution led to the formation of a pink crystalline solid. The solid was filtered off and washed with ether (40 mg, 66 %).

^{1}H NMR (500 MHz, CD_3CN, 300 K), δ (ppm): 167.13 (bs, 3H, H_{py}), 53.22 (s, 3H, H_{Py}), 41.04 (s, 3H, H_{Py}), 12.43 (bs, 6H, CH_2O), 10.17 (s, 6H, CH_2Py).

^{1}H NMR (500 MHz, CD_3OD, 300 K), δ (ppm): 160.83 (bs, 3H, H_{py}), 51.35 (s, 3H, H_{Py}), 41.76 (s, 3H, H_{Py}), 14.82 (bs, 6H, CH_2O), 11.08 (s, 6H, CH_2N).

ESI-MS in MeOH: m/z ($M = [Co^{II}$**TMPA^{CH2OH}**$]$ = $C_{21}H_{24}CoN_4O_3$ calc. 439.1180): 219.5578 (M^{2+} calc. 219.5576), 538.0634 ($[M + ClO_4]^+$ calc. 538.0660).

IR-ATR, drop casting from MeCN solution, $\overline{\nu}$ (cm^{-1}) = 3338.5 (O–H alcohol), 2940.9 (C–H aliphatic), 1609.0 (C=C py), 1105.1, 620.7 (ClO_4)

[Co^{II}(MeCN)Calix-TMPA^{OMe}](ClO$_4$)$_2$

Using a Schlenk tube under an argon flow, **Calix-TMPA^{OMe}** (50 mg, 37 μmol) was suspended in anhydrous deaerated MeCN (4 mL). $[Co^{II}(H_2O)_6](ClO_4)_2$ (15 mg, 41 μmol, 1.1 eq) and additional MeCN (2 mL) were then added. After overnight heating at 80 °C (the solution color changed from colorless to turquoise), and cooling back to room temperature, the reaction solution was layered with deaerated diethyl ether (30 mL) and left 2 hours. A turquoise solid then formed and was filtered off, washed with ether (5×5 mL), affording $[Co^{II}$(MeCN)**Calix-TMPA^{OMe}**$](ClO_4)_2$ (50 mg, yield: 80 %).

^{1}H NMR (500 MHz, CD_3CN, 300 K), δ (ppm): (500 MHz, CD_3CN, 298 K), 68.71 (3H, H_{Py}), 30.62 (3H, H_{Py}), 26.45 (3H, CH_3CN_{guest}), 7.57 (6H, H_{Ar}), 7.41 (6H, H_{Ar}), 3.59 (6H, $ArCH_2$), 3.27(6H, $ArCH_2$), 1.51 (27H, *t*Bu), 1.35 (27H, *t*Bu), 0.80 (6H, CH_2N), −1.78 (3H, H_{Py})

IR-ATR $[Co^{II}$(MeCN)**Calix-TMPA^{OMe}**$](ClO_4)_2$, drop casting from MeCN solution, $\overline{\nu}$ = 2960.3 (C–H aliphatic), 1654.6 (C=N pyridine), 1612.4, 1481.3 (py), 1109.1, 622.0 (ClO_4) cm^{-1}

ESI-HRMS: m/z ($M = [Co^{II}$**Calix-TMPA^{OMe}**$]$ = $C_{90}H_{108}CoN_4O_6$ = calc. 1399.7601): 720.3916 ($[M + MeCN]^{2+}$ calc 720.3916), 1416.7627 ($[M + OH]^+$ calc. 1414.7628), 1539.7346 ($[M + MeCN + ClO_4]^+$ calc. 1539.7351)

[Co^{II}(MeCN)Calix-TMPA^{OH}](ClO$_4$)$_2$

Under argon using a Schleck tube, **Calix-TMPA^{OH}** (33 mg, 25 μmol) was suspended in anhydrous deaerated MeCN (4 mL). A solution of $[Co(H_2O)_6][ClO_4]_2$ (10 mg, 26 μmol, 1.05 equiv.) dissolved in MeCN (1 mL) was then added, and the mixture was heated at 80 °C for 6 hours. The solution (initially pink) became turquoise and some solid precipitated out. After cooling (back to RT), the solution was layered by deaerated diethyl ether (15 mL). Turquoise needles were then obtained from the solution, filtered off and washed with ether (3×5 mL) affording $[Co^{II}$(MeCN)**Calix-TMPA^{OH}**$](ClO_4)_2$, (32 mg, yield: 81 %).

^{1}H NMR (500 MHz, $CD_3CN/CDCl_3$ 1 : 1 v/v), 300 K), δ (ppm): 66.48 (3H, s, H_{Py}), 31.31 (3H, s, H_{py}), 7.45 (6H, s, H_{Ar}), 7.35 (6 H, s, H_{Ar}), 3.59 (6H, s, ArCH), 3.15 (6H, s, ArCH), 1.47 (27H, s, *t*Bu), 1.42 (27H, s, *t*Bu), −1.07 (3H, s, H_{Py}).

^{1}H NMR (500 MHz, CD_3CN, 300 K), δ (ppm): 66.97 (s, 3H, H_{Py}), 31.59 (s, 3H, H_{Py}), 7.50 (s, 6H, H_{Ar}), 7.44 (s, 6H, H_{Ar}), 3.57 (s, 6H, $ArCH_2$), 3.18 (s, 6H, $ArCH_2$), 1.47 (s, 27H, *t*Bu), 1.45 (s, 27H, *t*Bu), −1.34 (s, 3H, H_{Py}).

IR-ATR $[Co^{II}$(MeCN)**Calix-TMPA^{OH}**$](ClO_4)_2$, drop casting from MeCN solution, $\overline{\nu}$ = 3328.5 (O–H phenol) 2957.1 (C–H aliphatic), 1613.9, 1481.0 (py), 1104.8, 1054.6 and 623.9 (ClO_4^-) cm^{-1}.

ESI-HRMS: m/z ($M = [Co^{II}$**Calix-TMPA^{OH}**$]$ = $C_{87}H_{102}CoN_4O_6$ = calc. 1357.7131): 699.3369 ($[M + MeCN]^{2+}$ calc. 699.3686), 1497.6852 ($[M + MeCN + ClO_4]^+$ calc. 1497.6876).

[Co^{II}(MeCN)Calix-TMPA^{Q}](ClO$_4$)$_2$

Calix-TMPA^{Q} (100 mg, 0.084 mmol) was solubilized by sonication and heating in acetonitrile (10 mL). $[Co^{II}(H_2O)_6]$ $(ClO_4)_2$ (35 mg, 0.095 mmol, 1.1 equiv.) was then added under Ar and the reaction mixture was heated at 70 °C in a closed tube for 22 h. The reaction was followed by ^{1}H NMR and stopped when no more protonated ligand was observed. The solvent was then removed *in vacuo* and the brown residue was suspended in 50 mL of CH_2Cl_2 and filtrated on celite to give a very dark brown solid and a yellow/green filtrate. The celite pad was washed two times with CH_2Cl_2. The filtrates were evaporated, dissolved into a minimum of CH_3CN, Et_2O was added and the precipitation was continued in the fridge (4 °C) overnight to yield the desired complex as a yellow solid (104 mg, 83 %).

^{1}H NMR (500 MHz, CD_3CN, 300 K), δ (ppm): 66.60 (s, 3H, H_{py}), 31.40 (s, 3H, H_{py}), 7.58 (s, 6H, H_{Ar}), 6.88 (s, 6H, H_Q), 3.28 (s, 6H, ArCH), 3.10 (s, 6H, ArCH) 1.59 (s, 27H, *t*Bu), −1.05 (s, 3H, H_{py}).

IR-ATR (cm^{-1}) drop casting from MeCN solution: $\overline{\nu}$ = 2968.0, 2901.1 (C–H aliphatic), 1654.7 (C=O quinone), 1612.5, 1579.12 (py), 1092.1, 623.7 (ClO_4^-) cm^{-1}

Research Article
doi.org/10.1002/ejic.202400228

ESI-HRMS: m/z (M = [Co^{II}**Calix-TMPA^{Q}**] = $C_{75}H_{72}CoN_4O_9$ = calc. 1231.4620): 636.2453 ([M + MeCN]$^{2+}$ calc. 636.2443), 1371.4378 ([M + MeCN + ClO_4]$^{+}$ calc. 1371.4371).

CCDC 2259825 ([Co^{II}**TMPA^{CH2OH}**]$(ClO_4)_2$) and CCDC2259838 ([Co^{II}(MeCN)**Calix-TMPA^{OMe}**][ClO_4]$_2$) contain supplementary crystallographic data for this paper. These data are provided free of charge by the joint Cambridge Crystallographic Data Centre and Fachinformationszentrum Karlsruhe at http://www.ccdc.cam.ac.uk/structures".

Supporting Information

The authors have cited additional references within the Supporting Information.[52–60] Complementary characterization data (spectra) and crystallography data can be found there.

Acknowledgements

NN thanks Ministère de l'Enseignement Supérieur et de la recherche and Université Paris Cité for a doctoral fellowship, and the CCCI funding from Université libre de Bruxelles. This research was supported by CNRS and Agence Nationale pour la Recherche (Marcel Project ANR-21-CE50-0034-02). Funding from Croatian Science Foundation through grant IP-2020-02-3786 (P.I.: Aleksandar Višnjevac) is gratefully acknowledged. Authors thank Annie Heroux (Elettra – Sincrotrone Trieste S.C.p.A.) for the data collection and Gael de Leener (Centre d'Instrumentation en REsonance Magnétique – CIREM, ULB) for helping with the NMR data analyses.

Conflict of Interests

The authors declare no conflict of interest.

Data Availability Statement

The data that support the findings of this study are available from the corresponding author upon reasonable request.

Keywords: Cobalt(II) · supramolecular · second coordination sphere · host-guest · nitrogen ligand

[1] J.-N. Rebilly, B. Colasson, O. Bistri, D. Over, O. Reinaud, *Chem. Soc. Rev.* **2015**, *44*, 467–489.
[2] O. Bistri, O. Reinaud, *Org. Biomol. Chem.* **2015**, *13*, 2849–2865.
[3] N. Le Poul, Y. Le Mest, I. Jabin, O. Reinaud, *Acc. Chem. Res.* **2015**, *48*, 2097–2106.
[4] P. Aoun, N. Nyssen, S. Richard, F. Zhurkin, I. Jabin, B. Colasson, O. Reinaud, *Chem. Eur. J.* **2023**, *29*.
[5] G. Izzet, X. Zeng, H. Akdas, J. Marrot, O. Reinaud, *Chem. Commun.* **2007**, 810–812.
[6] N. Nyssen, N. Giraud, J. Wouters, I. Jabin, L. Leherte, O. Reinaud, *Inorg. Chem. Front.* **2023**.
[7] G. Thiabaud, G. Guillemot, I. Schmitz-Afonso, B. Colasson, O. Reinaud, *Angew. Chem. Int. Ed.* **2009**, *48*, 7383–7386.
[8] N. Elgrishi, M. B. Chambers, X. Wang, M. Fontecave, *Chem. Soc. Rev.* **2017**, *46*, 761–796.
[9] D.-C. Liu, Z.-M. Luo, B. M. Aramburu-Trošelj, F. Ma, J.-W. Wang, *Chem. Commun.* **2023**, *59*, 14626–14635.
[10] L. Chen, G. Chen, C.-F. Leung, C. Cometto, M. Robert, T.-C. Lau, *Chem. Soc. Rev.* **2020**, *49*, 7271–7283.
[11] W. Xia, F. Wang, *Molecular Catalysis* **2023**, *535*, 112884.
[12] J. Bonin, A. Maurin, M. Robert, *Coord. Chem. Rev.* **2017**, *334*, 184–198.
[13] M. Usman, M. Humayun, M. D. Garba, L. Ullah, Z. Zeb, A. Helal, M. H. Suliman, B. Y. Alfaifi, N. Iqbal, M. Abdinejad, A. A. Tahir, H. Ullah, *Nanomaterials* **2021**, *11*, 2029.
[14] C. Li, X. Tong, P. Yu, W. Du, J. Wu, H. Rao, Z. M. Wang, *J. Mater. Chem. A* **2019**, *7*, 16622–16642.
[15] C. Cometto, L. Chen, P.-K. Lo, Z. Guo, K.-C. Lau, E. Anxolabéhère-Mallart, C. Fave, T.-C. Lau, M. Robert, *ACS Catal.* **2018**, *8*, 3411–3417.
[16] S. L.-F. Chan, T. L. Lam, C. Yang, J. Lai, B. Cao, Z. Zhou, Q. Zhu, *Polyhedron* **2017**, *125*, 156–163.
[17] S. L.-F. Chan, T. L. Lam, C. Yang, S.-C. Yan, N. M. Cheng, *Chem. Commun.* **2015**, *51*, 7799–7801.
[18] D. He, T. Jin, W. Li, S. Pantovich, D. Wang, G. Li, *Chem. Eur. J.* **2016**, *22*, 13064–13067.
[19] T. Ouyang, H. J. Wang, H. H. Huang, J. W. Wang, S. Guo, W. J. Liu, D. C. Zhong, T. B. Lu, *Angew. Chem. Int. Ed. Engl.* **2018**, *57*, 16480–16485.
[20] A. L. Ward, L. Elbaz, J. B. Kerr, J. Arnold, *Inorg. Chem.* **2012**, *51*, 4694–4706.
[21] E. Benazzi, F. Begato, A. Niorettini, L. Destro, K. Wurst, G. Licini, S. Agnoli, C. Zonta, M. Natali, *J. Mater. Chem. A* **2021**, *9*, 20032–20039.
[22] Z. Li, J.-D. Xiao, H.-L. Jiang, *ACS Catal.* **2016**, *6*, 5359–5365.
[23] Z.-J. Li, F. Zhan, H. Xiao, X. Zhang, Q.-Y. Kong, X.-B. Fan, W.-Q. Liu, M.-Y. Huang, C. Huang, Y.-J. Gao, X.-B. Li, Q.-Y. Meng, K. Feng, B. Chen, C.-H. Tung, H.-F. Zhao, Y. Tao, L.-Z. Wu, *J. Phys. Chem. Lett.* **2016**, *7*, 5253–5258.
[24] M. Natali, E. Badetti, E. Deponti, M. Gamberoni, F. A. Scaramuzzo, A. Sartorel, C. Zonta, *Dalton Trans.* **2016**, *45*, 14764–14773.
[25] J. Wang, C. Li, Q. Zhou, W. Wang, Y. Hou, B. Zhang, X. Wang, *Catal. Sci. Technol.* **2016**, *6*, 8482–8489.
[26] X. Guo, C. Li, W. Wang, Y. Hou, B. Zhang, X. Wang, Q. Zhou, *Dalton Trans.* **2021**, *50*, 2042–2049.
[27] T. J. Woods, M. F. Ballesteros-Rivas, S. Gómez-Coca, E. Ruiz, K. R. Dunbar, *J. Am. Chem. Soc.* **2016**, *138*, 16407–16416.
[28] C. J. Davies, G. A. Solan, J. Fawcett, *Polyhedron* **2004**, *23*, 3105–3114.
[29] S. S. Massoud, K. T. Broussard, F. A. Mautner, R. Vicente, M. K. Saha, I. Bernal, *Inorg. Chim. Acta* **2008**, *361*, 123–131.
[30] T. R. Lakshman, J. Deb, I. Ghosh, S. Sarkar, T. K. Paine, *Inorg. Chim. Acta* **2019**, *486*, 663–668.
[31] B. Chakraborty, I. Ghosh, R. D. Jana, T. K. Paine, *Dalton Trans.* **2020**, *49*, 3463–3472.
[32] B. Chakraborty, T. K. Paine, *Inorg. Chim. Acta* **2011**, *378*, 231–238.
[33] T. M. Kooistra, K. F. W. Hekking, Q. Knijnenburg, B. de Bruin, P. H. M. Budzelaar, R. de Gelder, J. M. M. Smits, A. W. Gal, *Eur. J. Inorg. Chem.* **2003**, *2003*, 648–655.
[34] S. S. Massoud, R. S. Perkins, F. R. Louka, W. Xu, A. Le Roux, Q. Dutercq, R. C. Fischer, F. A. Mautner, M. Handa, Y. Hiraoka, G. L. Kreft, T. Bortolotto, H. Terenzi, *Dalton Trans.* **2014**, *43*, 10086.
[35] W. Xu, F. R. Louka, P. E. Doulain, C. A. Landry, F. A. Mautner, S. S. Massoud, *Polyhedron* **2009**, *28*, 1221–1228.
[36] T. W. Failes, T. W. Hambley, *Dalton Trans.* **2006**, 1895–1901.
[37] P. Buglyó, I. Kacsir, M. Kozsup, I. Nagy, S. Nagy, A. C. Bényei, É. Kováts, E. Farkas, *Inorg. Chim. Acta* **2018**, *472*, 234–242.
[38] M. Kozsup, E. Farkas, A. C. Bényei, J. Kasparkova, H. Crlikova, V. Brabec, P. Buglyó, *J. Inorg. Biochem.* **2019**, *193*, 94–105.
[39] A. Nanthakumar, S. Fox, N. N. Murthy, K. D. Karlin, *J. Am. Chem. Soc.* **1997**, *119*, 3898–3906.
[40] Y. Li, S. Handunneththige, E. R. Farquhar, Y. Guo, M. R. Talipov, F. Li, D. Wang, *J. Am. Chem. Soc.* **2019**, *141*, 20127–20136.
[41] Y. Li, S. Handunneththige, J. Xiong, Y. Guo, M. R. Talipov, D. Wang, *J. Am. Chem. Soc.* **2020**, *142*, 21670–21678.
[42] G. Guisado-Barrios, Y. Li, A. M. Z. Slawin, D. T. Richens, I. A. Gass, P. R. Murray, L. J. Yellowlees, E. K. Brechin, *Dalton Trans.* **2008**, 551–558.
[43] A. B. P. Lever, *Inorganic Electronic Spectroscopy*, 2nd Edition, Elsevier, Amsterdam, **1984**.
[44] A. B. L. Banci, C. Benelli, R. Bohra, J.-M. Dance, D. Gatteschi, V. K. Jain, R. C. Mehrotra, A. Tressaud, R. G. Woolley, C. Zanchini, *Structures Versus Special Properties*, Springer, **1982**.

[45] O. Sénèque, M. Campion, M. Giorgi, Y. Le Mest, O. Reinaud, *Eur. J. Inorg. Chem.* **2004**, *2004*, 1817–1826.
[46] A. W. Addison, T. N. Rao, J. Reedijk, J. Van Rijn, G. C. Verschoor, *J. Chem. Soc. Dalton Trans.* **1984**, 1349–1356.
[47] D. F. Evans, *Journal of the Chemical Society (Resumed)* **1959**, 2003–2005.
[48] C. J. Bond, G. E. Sokolow, M. R. Crawley, P. J. Burns, J. M. Cox, R. Mayilmurugan, J. R. Morrow, *Inorg. Chem.* **2019**, *58*, 8710–8719.
[49] R. Evans, Z. Deng, A. K. Rogerson, A. S. McLachlan, J. J. Richards, M. Nilsson, G. A. Morris, *Angew. Chem. Int. Ed.* **2013**, *52*, 3199–3202.
[50] P. B. Tsitovich, J. M. Cox, J. B. Benedict, J. R. Morrow, *Inorg. Chem.* **2016**, *55*, 700–716.
[51] T, Koen, Q. Knijnenburg, Bas, Peter, René, Jan, Anton, *Eur. J. Inorg. Chem.* **2003**, *2003*, 648–655.
[52] Z. He, P. J. Chaimungkalanont, D. C. Craig, S. B. Colbran, *J. Chem. Soc. Dalton Trans.* **2000**, 1419–1429.
[53] U. Darbost, M.-N. Rager, S. Petit, I. Jabin, O. Reinaud, *J. Am. Chem. Soc.* **2005**, *127*, 8517–8525.
[54] U. Mueller, M. Thunnissen, J. Nan, M. Eguiraun, F. Bolmsten, A. Milàn-Otero, M. Guijarro, M. Oscarsson, D. de Sanctis, G. Leonard, *Synchrotron Radiation News* **2017**, *30*, 22–27.
[55] W. Kabsch, *Acta Crystallogr. Sect. D* **2010**, *66*, 125–132.
[56] G. M. Sheldrick, *Acta Crystallogr A Found Adv* **2015**, *71*, 3–8.
[57] C. F. Macrae, I. J. Bruno, J. A. Chisholm, P. R. Edgington, P. McCabe, E. Pidcock, L. Rodriguez-Monge, R. Taylor, J. Van De Streek, P. A. Wood, *J. Appl. Crystallogr.* **2008**, *41*, 466–470.
[58] A. L. Spek, *Acta Crystallogr. Sect. D* **2009**, *65*, 148–155.
[59] L. J. Farrugia, *J. Appl. Crystallogr.* **1999**, *32*, 837–838.
[60] C. R. Groom, I. J. Bruno, M. P. Lightfoot, S. C. Ward, *Acta Crystallogr B Struct Sci Cryst Eng Mater* **2016**, *72*, 171–179.

Manuscript received: April 22, 2024
Revised manuscript received: May 16, 2024
Accepted manuscript online: May 17, 2024
Version of record online: July 19, 2024